in vivo *38*: 2300-2309 (2024)
doi:10.21873/invivo.13695

Amine Oxidase, Copper Containing 3 (*Aoc3*) Knockout Mice Are More Prone to DSS-induced Colitis and Colonic Tumorigenesis

ÖZGE ÖZCAN[1], ÖZGE AKYOL[2] and AYTEKIN AKYOL[2,3,4]

[1]*Department of Stem Cell Sciences, Graduate School of Health Sciences, Hacettepe University, Ankara, Turkey;*
[2]*Department of Pathology, Hacettepe University Faculty of Medicine, Ankara, Turkey;*
[3]*Hacettepe University Transgenic Animal Technologies Research and Application Center, Ankara, Turkey;*
[4]*Molecular Pathology Application and Research Center, Hacettepe University, Ankara, Turkey*

Abstract. *Background/Aim: Inflammatory bowel diseases and colorectal cancer are a major cause of morbidity and mortality. Amine oxidase, copper-containing 3 (AOC3) is a critical enzyme in the physiological trafficking of leukocytes and the regulation of inflammation. This study aimed to examine the effects of Aoc3 deficiency in mice models of colitis and colorectal tumorigenesis. Materials and Methods: C57BL/6 and Aoc3 knockout mice were used for Dextran Sodium Sulfate (DSS) induced acute colitis and the Azoxymethane (AOM)/DSS model of inflammation-related colon cancer. We also evaluated the effect of Aoc3 in an Apc mutant mice model of intestinal and colonic tumorigenesis. Results: We observed that Aoc3 deficient mice were more prone to colitis induced by DSS in early phases and their survival was shorter. We also showed that Aoc3 deficient mice developed more tumors both in AOM/DSS and Apc mutant mice models. Furthermore, colonic tumors in the AOM/DSS groups in Aoc3 mutant mice were generally invasive type adenocarcinomas. Conclusion: Aoc3 deficiency promotes colitis and colonic tumorigenesis in mouse models.*

Ulcerative colitis and Crohn's disease are called inflammatory bowel diseases (IBDs), and are an important cause of major morbidity (1). Although IBDs are diseases with well-defined clinical, endoscopic and morphological features, their etiology and pathogenesis have not yet been fully elucidated. Many factors, such as the genetic predisposition of affected individuals, immune system, intestinal microbiota, nutritional habits, and environmental factors can affect the underlying disease process (2). Tissue damage due to excessive inflammation can cause complications related to both structural and neoplastic processes. IBD patients are at increased risk for the development of colorectal cancer (CRC) (3). The pathogenesis of CRC and the affected signaling pathways have been studied in great detail, and tumors develop as a result of alterations in signaling pathways, such as Wnt, TGF, TP53, PI3K, and RTK-Ras (4). Chronic colonic inflammation caused by infections, dysregulated immune responses, IBDs, or environmental factors can initiate and promote the inflammation-related CRC development. Although it is well known that inflammation facilitates tumor progression, the underlying pathogenesis of this process still requires further investigation to be fully defined (3).

Amine oxidases are a group of enzymes that control the oxidation of some important biologically active amines present in all living systems. Due to their pivotal role, they have been the focus of research related to human diseases (5). One important subgroup of amine oxidases are copper amine oxidases (CAOs), which need Cu^{+2} and a tyrosine-derived quinone cofactor to generate other biologically active molecules from amines, such as hydrogen peroxide and ammonia. The byproducts of these enzymes either directly or indirectly influence tissues and regulate inflammation, fibrosis, tumor invasion, and other disease processes (6). Amine oxidase, copper-containing 3 (AOC3)/vascular adhesion protein-1 (VAP-1), also called as semicarbazide-sensitive amine oxidase (SSAO) is mainly expressed in the lung, aorta, and liver, but it can also be found in adipocytes, smooth muscle cells, and endothelial cells. It is involved in

Correspondence to: Aytekin Akyol (ORCID: 0000-0002-4075-3475), MD, Professor of Pathology, Hacettepe University Department of Pathology, Sihhiye, 06100, Ankara, Turkey. Tel: +90 3123051555, e-mail: aytekina@hacettepe.edu.tr

Key Words: Inflammatory bowel disease, Aoc3, colitis, colon cancer.

Table I. *Primers that were used for mice genotyping and expected amplicon sizes.*

	Multiplex PCR primer sequences (5'→3')		
	Forward	Reverse	Amplicon size
$Apc^{+/+}$	CAGCAGCTTTAAGGAATCTCA	TCTGACCTACTATCATCATGTCG	268 bp
$Apc^{+/-}$	GTCTGCCATCCAGGAAA	TCTGACCTACTATCATCATGTCG	185 bp
$Aoc3^{+/+}$	GCCCACAAGGAAGAAGACAC	CAAACACCAGGGACAGAACC	405 bp
$Aoc3^{-/-}$	GGCTGCTGATCTCGTTCTTC	TCTGGATTCATCGACTGTGG	604 bp

leukocyte trafficking between blood and tissues under physiological and pathological conditions. AOC3 catalyzes the oxidative deamination of primary amines in a reaction that produces aldehyde, ammonium, and hydrogen peroxide (7). The absence of AOC3 leads to a decrease in lymphocyte traveling to the lymphoid organs and reduced AOC3 levels attenuate the inflammatory response in peritonitis (8). The soluble form of it is released by degradation with metalloproteinases and its circulating level is known to be increased in rheumatoid arthritis, inflammatory bowel diseases, and inflammatory liver diseases (9). However, knowledge on the expression of tissue-dependent Aoc3 and soluble Aoc3 in CRCs (10, 11) and IBDs is very limited (12).

The dextran sulfate sodium (DSS)-induced colitis (13, 14) and inflammation-related mouse colon carcinogenesis model induced by azoxymethane and dextran sodium sulfate (AOM/DSS) (15) are well studied animal models. In mice, acute and chronic colitis may be induced with oral administration of 2-5% DSS in drinking water for different time periods based on the experimental procedure. Because of that, dose optimization for different experiments and DSS batches from different vendors should be performed before specific experiments (16). Murine models of CRCs are a very well studied subject, based on specific underlying molecular mechanisms of CRCs (17). Most of these models target and modify the mouse *Apc* gene in different experimental approaches (18). Association of *Apc* mutation and colitis is also well studied in mouse models in the context of colon cancer development (19).

Although the role of Aoc3 in inflammatory diseases is very well studied, its role in IBDs and CRCs has not been studied in preclinical disease models. In addition to that, since Aoc3 is a potential treatment target (20), it increases the importance of knowing its role in inflammatory and neoplastic diseases of the colon. Therefore, this study aimed to elucidate the effect of Aoc3 in mouse models of colitis and colon cancer.

Materials and Methods

Mouse colony, genotyping and establishment of experimental cohorts. Mice homozygous for a null mutation of $Aoc3^{-/-}$ were previously described (8) and donated by Dr. Sirpa Jalkanen as a kind gift from the University of Turku. $Apc^{+/-}$ mutant mice with an 8-nucleotide deletion at codon 750 were generated in our laboratory using the CRISPR/Cas9 system. These mice have been used as a model for intestinal and colon polyposis in previous studies (21). Genotyping of *Aoc3* and $Apc^{+/-}$ mutant mice was performed with multiplex polymerase chain reaction (PCR) from genomic tail DNA isolated from each mouse and primer sequences are shown in Table I. In order to establish $Aoc3^{-/-}$, $Aoc3^{+/-}$, and $Aoc3^{+/+}$ mice in the $Apc^{+/-}$ background, $Aoc3^{+/-}$ mice were mated with $Apc^{+/-}$ mice. All mice were housed in individually ventilated cages under the standard 12 h light and 12 h dark cycle, at room temperature, *ad-libitum* feeding with standard diet and water. All experimental procedures were carried out in accordance with the regulations of Hacettepe University Animal Experimentations Ethics Board (Approval number: 2020/60).

Chemicals, induction of colitis and colitis-induced tumorigenesis. Acute colitis induction was performed by using DSS in drinking water (TdB Consultancy AB, Uppsala, Sweden). In order to determine the optimal dose for induction of acute colitis, C57BL/6 (wild-type, WT) and Aoc3–/– mice were treated with 2%, 2.5%, and 3% DSS for five days. For the experimental cohorts of acute colitis, 2.5% DSS was administered for 8 days and animals were terminated on the 9th day. In colitis induction experiments, all mice were weighted daily; stool consistency and rectal bleeding were also evaluated. AOM/DSS was used for the colitis-induced tumor model. In this model, mice were treated 10 mg AOM (Sigma-Aldrich, St. Louis, MO, USA) per kg body weight with intraperitoneal injection at the beginning, followed by 5 days with drinking water containing 2% DSS. After that normal drinking water was provided for the next 9 days. This regimen (2% DSS and normal drinking water) repeated for 3 cycles. Afterward, all animals were provided with normal drinking water until termination at the 14th week for dissection and analysis of colonic tumors.

Dissection of mice, polyp counting and collection of tissue samples and histopathological assessment of colitis. All experimental groups were sacrificed under anesthesia and dissections were performed. The entire gastrointestinal tract was removed and put into 1X PBS at +4°C for the experimental groups in which DSS was applied. Then, the colon from the anus to the cecum was opened longitudinally and washed with 1X PBS. The opened specimens were photographed and the length of the colons was measured. In the cohort that was formed with $Apc^{+/-}$ and $Aoc3^{+/-}$ mice matings, the entire gastrointestinal tract was removed and opened. The samples were fixed in 10% buffered formalin. One day later, the

formalin-fixed samples were examined under a stereo microscope (ZEISS Stemi 305 Model Stereomicroscope, Carl Zeiss AG) for colonic polyp counts. The number and location of polyps were recorded. After this, the entire colon was used to prepare formalin-fixed paraffin-embedded (FFPE) blocks to make H&E sections for histomorphological analysis. H&E-stained slides of colon samples were evaluated for histological activity score of colitis based on three parameters: the severity of inflammation, crypt damage, and ulceration. Severity of inflammation was scored as 0 to 3 (rare to transmural extension of the inflammatory infiltrate). Crypt damage was scored as 0 to 5 (intact crypts to confluent erosion) and ulceration was scored as 0 to 3 (absence of ulcer to confluent or extensive ulceration). The scores were summed up to obtain a histological activity score ranging 0-11, as described previously (22). Other internal organs of sacrificed mice were also evaluated histomorphologically under a light microscope.

Total RNA isolation, cDNA synthesis, and qPCR analysis on colon epithelium samples. Fresh distal colon samples from C57BL/6 and *Aoc3*$^{-/-}$ mice were collected into the RNAlater solution (Thermo Fisher Scientific, Waltham, MA, USA) and stored at –80˚C. Total RNA extraction was performed by TRIzol reagent (Thermo Fisher Scientific). RNA clean-up was done using the Qiagen RNeasy Kit (Qiagen, Germantown, MD, USA) as instructed in the vendors' manual. cDNA synthesis from total RNA was performed by using the High-Capacity cDNA Reverse Transcription kit (Thermo Fisher Scientific) with random primers. qPCR experiments were performed with the Stratagene Mx3005P thermocycler system (Agilent Technologies, Palo Alto, CA, USA). Forward (F) and Reverse (R) primers (5'-3' sequence) for *Aoc3* (F:GTGGTCAGAT CCGTGTCTACCTT and R:CCTGTGGCGTGGAATTTGA) and *Actb* (F:AGCCATGTACGTAGCCATCC and R:CTCTCAGCT GTGGTGGTGAA) were used. For the qPCR reaction, Luminaris Color HiGreen Low ROX qPCR Master Mix (Thermo Scientific, LSG-K0373) kit was used as the vendor's manual. All reactions were performed in triplicate, and relative expression levels were determined by the ΔCT method. The $2^{-\Delta\Delta Ct}$ method was used to calculate the relative fold gene expression of the samples.

BrdU assay. Proliferation in tumor tissues was examined by using BrdU labeling. Mice to be tested were weighed, and BrdU (BrdU (5-Bromo-2´-Deoxyuridine, Catalog number: B23151, Invitrogen, Thermo Fisher Scientific) was injected intraperitoneally at the appropriate dose according to their body weight (100 mg/kg). Dissection was performed 1 h after injection and then histological sample sections were prepared from the gastrointestinal tract. Unstained sections from FFPE blocks were immunostained with anti-BrdU antibody (BrdU Polyclonal Antibody, Catalog # PA5-32256, invitrogen, Thermo Fisher Scientific) as described in detail (21).

Statistical analysis. Descriptive analyses were presented as mean and standard error of mean. Differences between the two groups were compared using the *t*-test. Survival analyses were performed using the Kaplan-Meier method and the survival curves were compared for time-to-event measures with a log-rank test. *p*-Value <0.05 was used to infer statistical significance. Sample size estimates were not used. GraphPad Prism version 10.2.1 (GraphPad Software Inc.) for Windows was used for statistical analyses.

Results

Aoc3 knockout mice, genotyping, histological analysis, and gene expression. Multiplex PCR results confirmed the genotypes of C57BL/6 wild-type (wt), *Aoc3* heterozygous and knockout mice (Figure 1A). Histological evaluation of the internal organs and gastrointestinal tract of these three groups of mice did not show any specific finding. Histological staining of the colon of *Aoc3*$^{-/-}$ and wt mice is shown in Figure 1B and C, respectively. *Aoc3* expression was examined using qPCR and found to be 5-fold lower in *Aoc3*$^{-/-}$ mice when compared to wt mice (Figure 1D).

Optimisation of DSS dose for the induction of acute and chronic colitis in C57BL/6 and Aoc3 knockout mice. A preliminary experiment was conducted to determine which of 2%, 2.5% and 3% DSS concentrations was optimal for the induction of acute and chronic colitis (n=2 for each group for both wt and *Aoc3*$^{-/-}$ mice). The severity of colitis was evaluated by assessing weight loss, rectal bleeding, colon length, and histological activity index. The weight loss of the mice was between 10-15%, stool was watery, and bleeding was evident in both wt and *Aoc3*$^{-/-}$ groups administered 3% DSS. All animals were sacrificed after six days of follow-up and colon lengths were compared. The colon length shortened with increasing DSS concentration in both wt and *Aoc3*$^{-/-}$ mice (Figure 1E and F). At the same time, increasing DSS concentrations caused increased weight loss in both cohorts. Wt and *Aoc3*$^{-/-}$ mice given 3% DSS started to lose weight rapidly after day 4 (Figure 1G). Histological activity score including inflammation severity, crypt damage, and ulceration were also found to be higher with increasing DSS concentration. It was also observed that *Aoc3*$^{-/-}$ mice were more prone to acute colitis (Figure 1H). Since 3% DSS caused severe colitis, which was more prominent in the *Aoc3*$^{-/-}$ group, 2.5% DSS was used for the subsequent acute colitis experiments (Figure 1I-K). 2% DSS was chosen for the long-term induction for tumorigenesis experiments using the AOM/DSS colitis model.

Aoc3 knockout mice showed shorter survival in acute colitis experiments. In acute colitis experiments, C57BL/6 wild-type mice and Aoc3 knockout mice (n=4 male mice in each group) were administered 2.5% DSS in drinking water and the similar age and body weight-matched control group was administered normal drinking water. Mice were followed for nine days and those treated with 2.5% DSS showed rapid weight loss starting from day 4. *Aoc3*$^{-/-}$ mice treated with 2.5% DSS showed more weight loss compared with C57BL/6 wild-type mice (Figure 2A). Furthermore, rectal bleeding started on day 4 (Figure 2B). In survival analysis, three of the C57BL/6 wild-type mice (n=4) in the 2.5% DSS group died on day 8 and only 1 mouse survived until day 9 in an acute

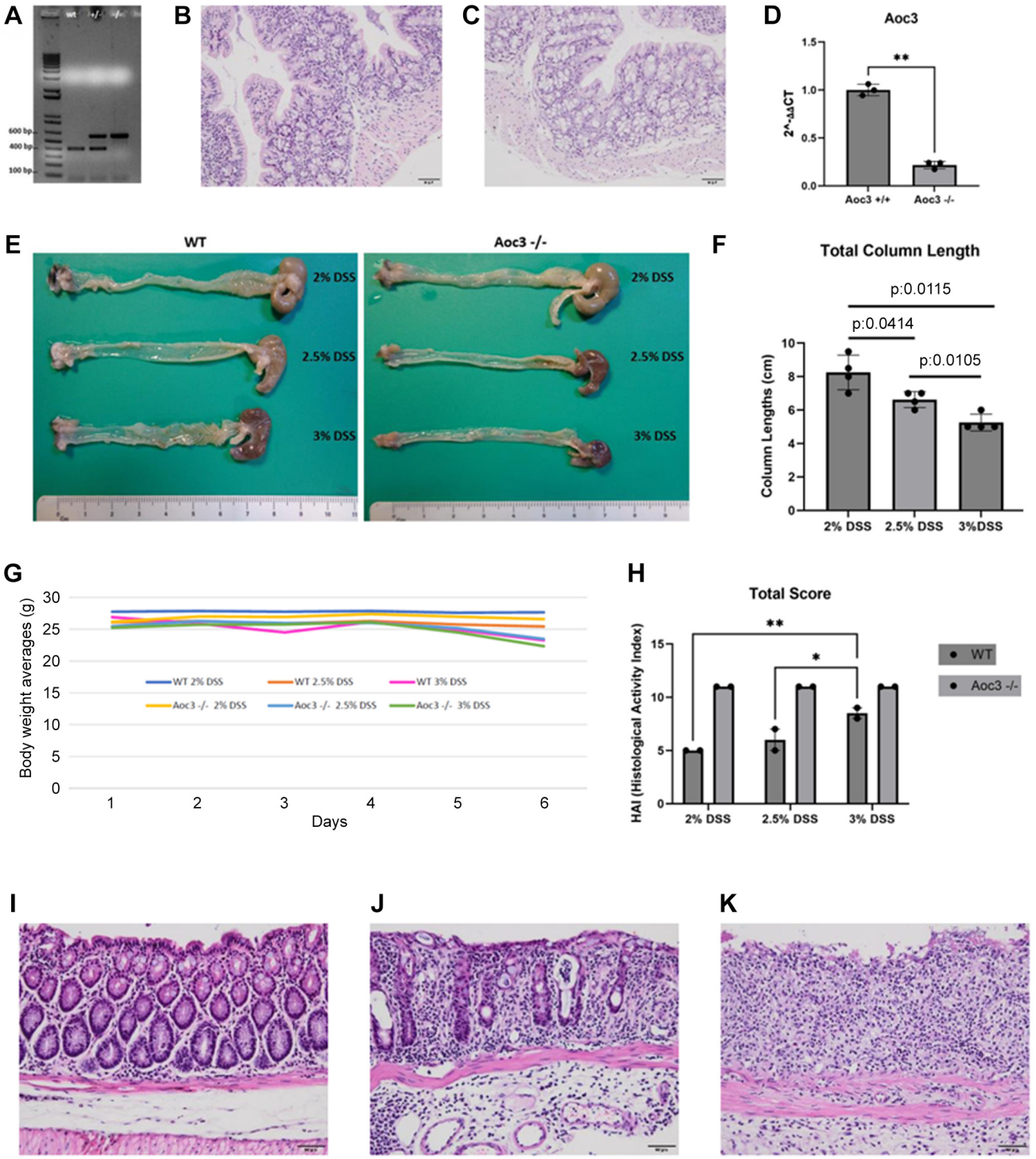

Figure 1. *Aoc3 knockout mice genotyping-phenotyping, Aoc3 expression in distal colon and optimization of dextran sulfate sodium (DSS) concentration for colitis induction. Genotyping of Aoc3 wild-type (wt), heterozygous and knockout mice by multiplex PCR (A). Histological examination of colon revealed no difference between C57BL/6 wt and Aoc3$^{-/-}$ mice, respectively (B-C). Comparison of Aoc3 expression in wild type and Aoc3$^{-/-}$ mice (normalized to housekeeping gene Actb) (t-test, p-Value=0.0048) (D). Colon lengths shortened with increasing DSS concentration (2%, 2.5% and 3% DSS) in both wt and Aoc3$^{-/-}$ mice (E-F). Body weight loss is also more prominent in higher concentrations of DSS in drinking water (G). Histologic activity index (HAI) increased in parallel with increasing DSS dose (2%, 2.5% and 3%, respectively) in wild-type mice groups. In Aoc3 mice, HAI was at maximum score at all doses and was relatively higher in their control wild-type groups (H). H&E representative images of the distal colon from control, 2.5% DSS-treated wt, and 2.5% DSS-treated Aoc3$^{-/-}$ mice, respectively (I-K). Scale bars: 50 μm.*

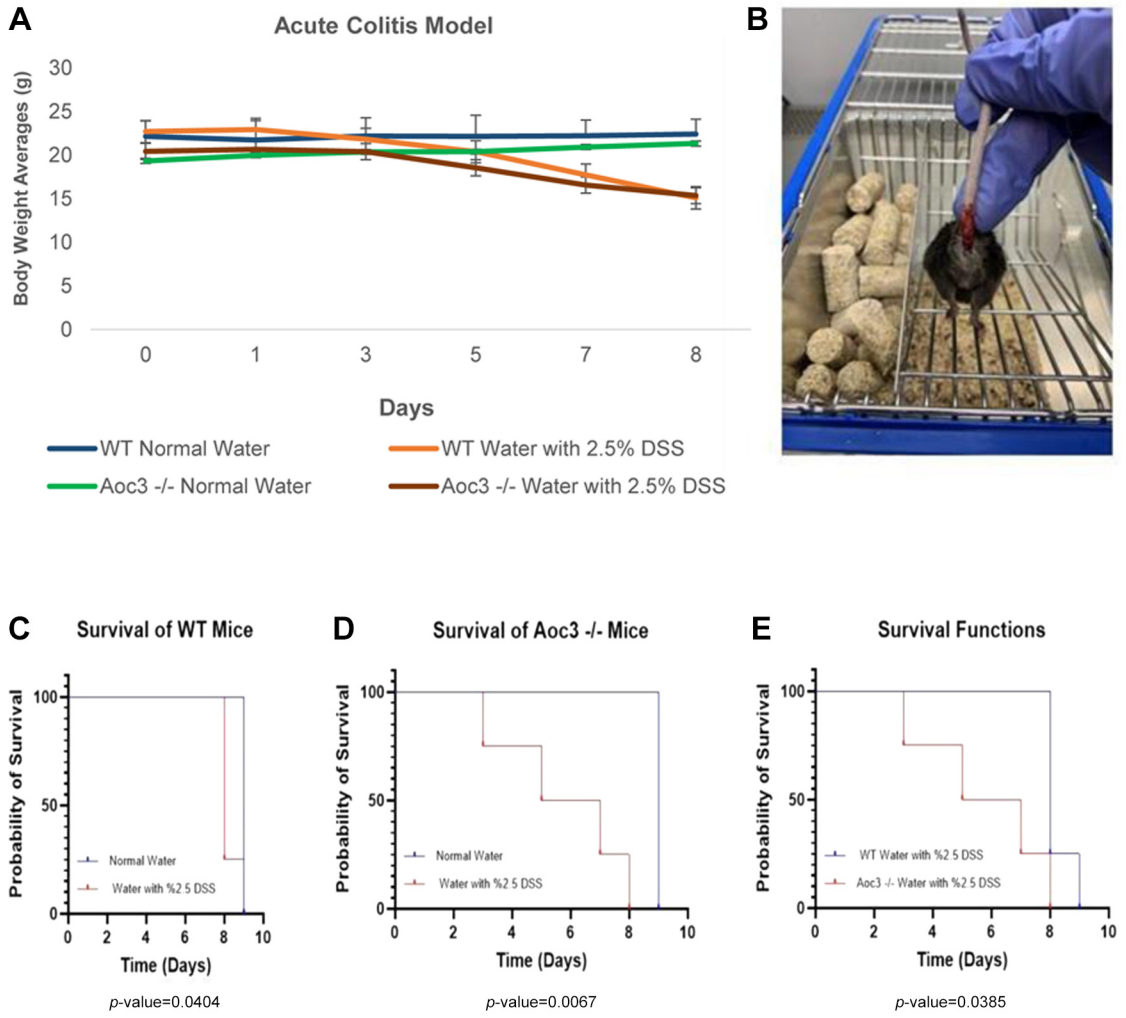

Figure 2. *Acute colitis in wild-type (wt) and Aoc3$^{-/-}$ mice. Graph of mean body weights of mice followed for 9 days (A) and image of rectal bleeding on day 4 (B). Kaplan-Meier curves showing the survival of the experimental groups during the 9 days follow-up. Survival curves for wt (C), Aoc3$^{-/-}$ (D) and comparisons of wt and Aoc3$^{-/-}$ mice given 2.5% dextran sulfate sodium (E). *p<0.05, Kaplan-Meier analysis, log-rank test.*

colitis experiment. All mice in the control group (n=4) given normal drinking water survived until the end of the experiment (Figure 2C). When the survival of *Aoc3*$^{-/-}$ mice (n=4) in the 2.5% DSS group was examined, it was observed that all mice died starting from day 3 until day 8, while all of the *Aoc3*$^{-/-}$ mice (n=4) in this group given normal drinking water survived until the end of the experiment (Figure 2D). It was found that *Aoc3*$^{-/-}$ mice were more affected by DSS-induced acute colitis than C57BL/6 wild-type mice (p value=0.0385) (Figure 2E). Since almost all mice were dead at the end of the experimental follow-up, no further colon length and histological activity could be evaluated.

AOM/DSS induction caused more colonic tumors which were mostly invasive adenocarcinomas in Aoc3 knockout mice. In colitis-induced tumorigenesis experiments, C57BL/6 wild-type (n=28) and *Aoc3* knockout (n=36) mice were subdivided into four groups (0.9% NaCl control: n=6 and n=9; only AOM: n=8 and n=9; only 2% DSS: n=7 and n=9; and AOM+2% DSS: n=7 and n=9; wt and *Aoc3* knockout mice numbers in each subgroup; respectively). The experimental strategy is demonstrated in Figure 3A. *Aoc3*$^{-/-}$ mice treated with AOM/DSS and 2% DSS started losing body weight after the 3rd week (Figure 3B). Only 2% DSS and AOM/DSS administration resulted in more colonic tumor formation in *Aoc3*$^{-/-}$ mice compared to wt controls (Figure 3C). Regarding survival, wt mice treated with AOM/DSS started to die from day 150, whereas *Aoc3*$^{-/-}$ mice started to die from day 75. Regarding DSS-treated groups (both only 2% DSS and AOM/DSS), all of the 14 mice in the C57BL/6 group

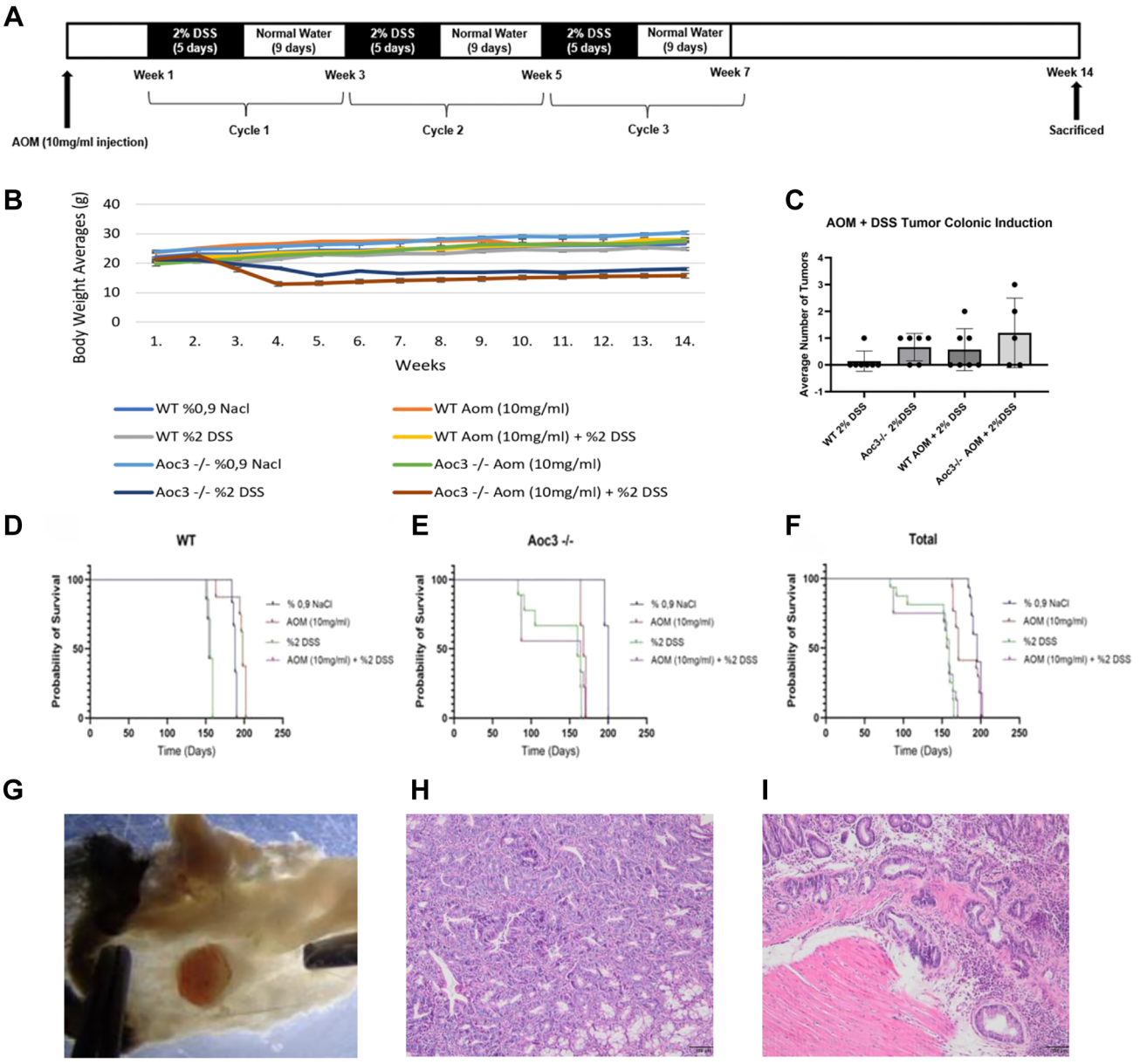

Figure 3. *Experimental protocol for colitis-induced tumor model generated by the administration of azoxymethane/dextran sodium sulfate (AOM/DSS) (A). Body weight follow up and column scatter plots of the experimental groups. Average body weight of female mice in the experimental groups (B). Comparison of colonic tumor numbers of wt and Aoc3$^{-/-}$ mice treated with 2% DSS or AOM/DSS (C). Kaplan-Meier curves showing the survival of the experimental groups during the 14-week follow-up of WT, Aoc3$^{-/-}$, all groups, respectively (D-E). *p<0.05, Kaplan-Meier analysis, log-rank test. Macroscopic image of distal colonic tumor (G) and H&E staining image of colonic adenoma from AOM/DSS-treated wt mice (H) and invasive adenocarcinoma from AOM/DSS-treated Aoc3$^{-/-}$ mice (I). Scale bars: 100 μm.*

survived until the end of the experimental period, while 12 mice out of 18 (67%) survived in the *Aoc3*$^{-/-}$ group. This showed that *Aoc3*$^{-/-}$ mice were highly affected by AOM/DSS administration (Figure 3D-F). Macroscopic examination revealed distal colonic tumors (Figure 3G). Microscopic histologic examination of the whole colon dissected from wt groups demonstrated 5 tumors of which four were adenoma and one was invasive adenocarcinoma (Figure 3H). Of the 10 colonic tumors present in AOM+DSS treated *Aoc3*$^{-/-}$ mice groups three were adenoma and seven invasive adenocarcinoma (Figure 3I).

Aoc3 deficient mice are more prone to colonic tumorigenesis in the germline Apc mutant intestinal-colonic mice tumor

Table II. *Mean number of intestinal and colonic polyps in Apc and Aoc3 mutant mice. SD: Standard deviation, SE: standard error.*

Sex	Genotype & number (n)	Mean number of intestinal polyps (SD-SE)	Mean number of colon polyps (SD-SE)
Male	$Apc^{+/-}$ $Aoc3^{-/-}$ n=4	56.00 (28.30-0.51)	13.25 (5.32-0.40)
Male	$Apc^{+/-}$ $Aoc3^{+/-}$ n=3	24.33 (7.64-0.31)	8.67 (3.21-0.37)
Male	$Apc^{+/-}$ $Aoc3^{+/+}$ n=3	31.67 (15.00-0.48)	6.00 (2.64-0.44)

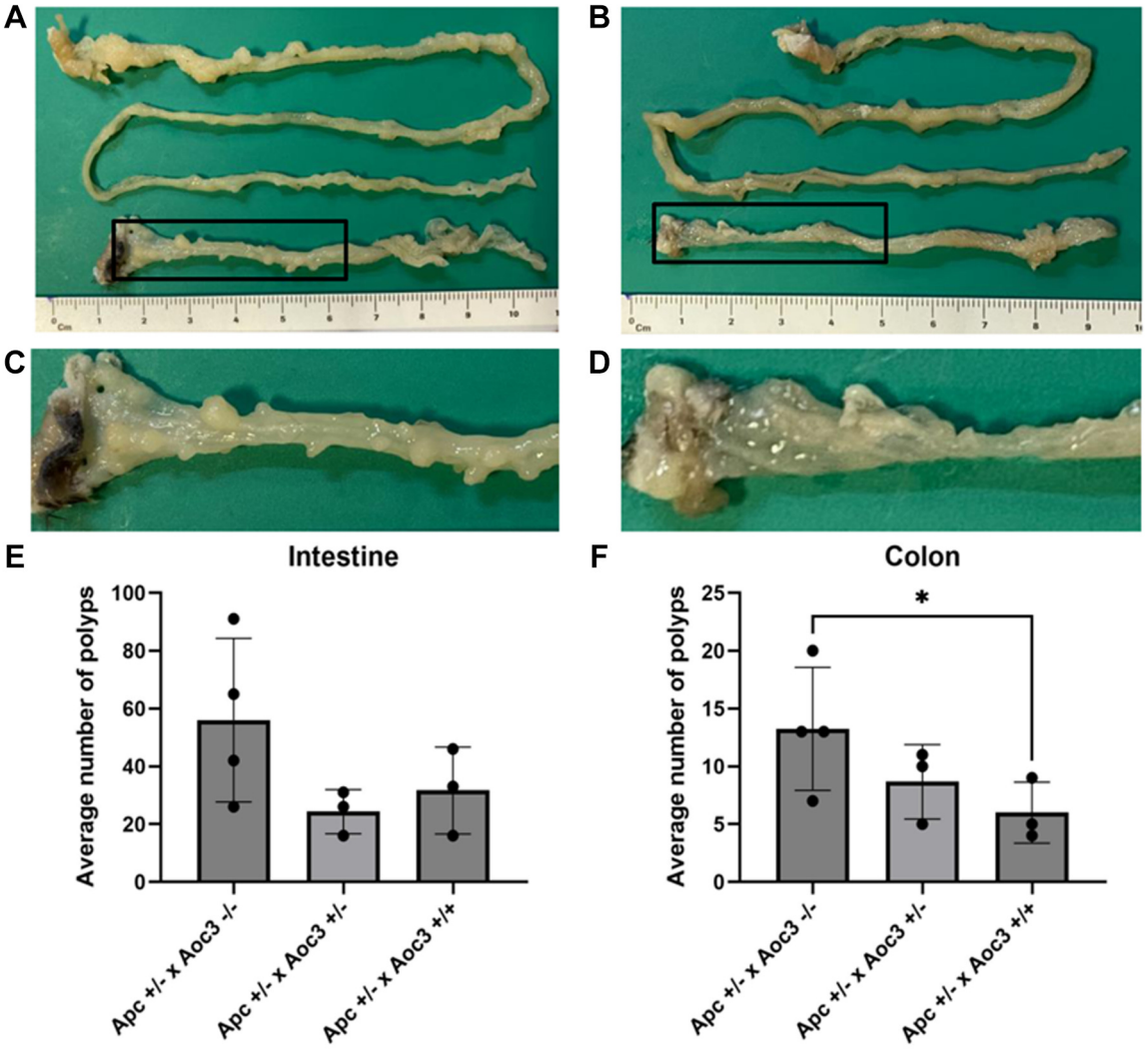

Figure 4. *Macroscopic images of the whole gastrointestinal tract of $Apc^{+/-}$ $Aoc3^{-/-}$ and $Apc^{+/-}$ $Aoc3^{+/+}$ mice (A, B) and images of the distal colon (C, D), respectively. Average number of small intestine (E) and colon polyps (F) in Apc mutant mice with Aoc3 mutational status (homozygous mutation or heterozygous mutation or wild-type, respectively).*

model. In order to test the effect of Aoc3 knockout on intestinal and colonic tumorigenesis in the *Apc* mutant mice, we formed three groups and animals in each group were followed for 18 weeks. After that, all mice were sacrificed and the number of polyps in the intestine and colon are shown in Table II. *Aoc3* knockout mice developed more

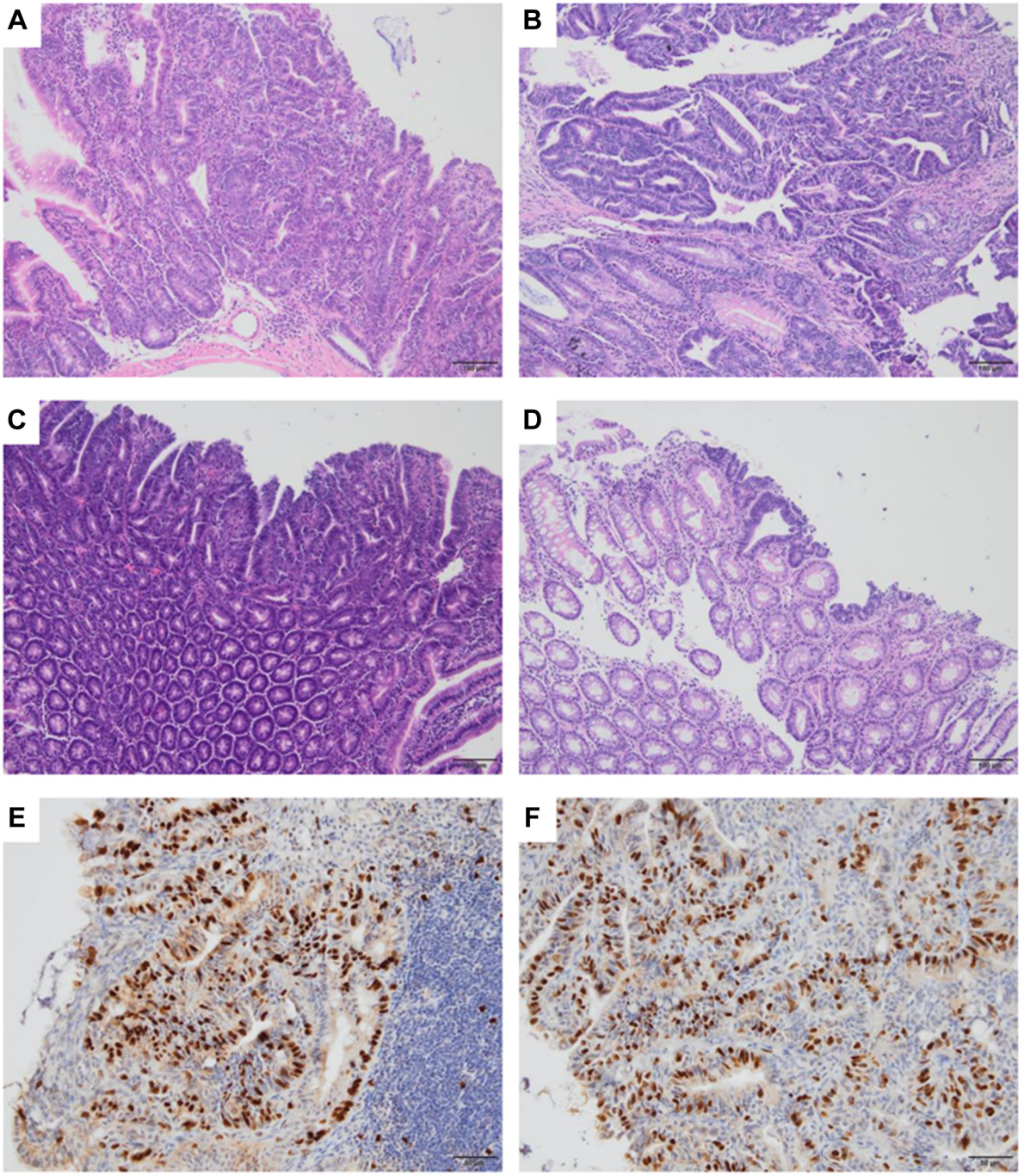

Figure 5. *H&E staining of small intestinal adenomas (A, B), colonic polyps (C, D) and BrdU labeling of small intestinal adenomas (E, F) from* $Apc^{+/-}$ $Aoc3^{-/-}$ *and* $Apc^{+/-}$ $Aoc3^{+/+}$ *mice are presented, respectively. Scale bars: 100 μm and 50 μm.*

intestinal and colonic tumors (Figure 4A-F). Tumors showed histologically adenomatous morphology in both the intestine and colon (Figure 5A-D). Brdu labelling showed similar proliferation activity in both wt and *Aoc3* knockout mice polyps (Figure 5E and F).

Discussion

In this study, we showed that the absence of Aoc3 promotes tumor progression in AOM/DSS-induced colonic tumor and Apc mutant intestinal/colonic tumor model in mice. We also

demonstrated that Aoc3 deficient mice are more prone to DSS-induced colitis than wild-type C57BL/6 mice.

In the last decades, Aoc3 has been considered a novel clinical biomarker and a potential therapeutic target for inflammatory disorders (23). Studies related with Aoc3 mostly focused on its role in vascular inflammatory diseases (24), atherosclerosis (25, 26), coronary heart disease (27), liver fibrosis (9, 28) and metabolic disorders (29). Although detailed studies have been conducted on many diseases accompanied by inflammatory processes, there are not many studies on the role of Aoc3 in the development of IBDs and CRCs. In one of the rare articles, it was shown that the serum level of soluble AOC3/VAP1 in patients with colon cancer decreased (10). Our own observation of AOC3 down-regulation in CRCs samples is also supported by this finding (unpublished data). Another study reported that AOC3 may be an activation marker for cancer-associated fibroblasts and may have a role in CRC progression (11).

Inflammatory diseases like rheumatoid arthritis and IBDs were not associated with elevated sVAP-1 levels (9). Similar to this study, Koutroubakis *et al*. have found that sVAP-1 serum concentrations were not significantly different between 161 IBD patients (90 ulcerative colitis, 71 Crohn's disease) and 93 healthy controls (12). Although the pathogenesis of IBD is not fully known, the relationship of intestinal stromal cells with the disease has been frequently emphasized recently (30). Another study also showed that AOC3 is a marker for pericryptal myofibroblasts in the colon and rectum (31). Our observation also supports this finding (unpublished data). In this study we demonstrated that in a *in vivo* model Aoc3 deficiency is associated with colitis and CRCs development. However, elucidation of the mechanism of pathogenesis requires further studies.

Aoc3 modulation, especially inhibition, is used as an treatment alternative in diseases where inflammation is involved in the pathogenesis (20). There are many preclinical and clinical studies are ongoing in this field as a target molecule for treatment of such diseases (7). Treatment of a mouse model of chronic obstructive pulmonary disease with the inhibitor of semicarbazide-sensitive amine oxidase PXS-4728A improved lung function by suppressing airway inflammation and fibrosis (32). In a Phase II study, the AOC3 inhibitor BI 1467335 dose-dependently reduced serum ALT and CK-18 caspase in adults with non-alcoholic steatohepatitis (33). In our study, we showed that the deficiency of AOC3 promoted the progression of both colitis and CRC, in contrast to the inflammatory diseases in the literature. Because of that, restoring the function of AOC3, not inhibition, may be used as a treatment modality in IBDS and CRCs. Therefore, AOC3 activation needs to be further studied experimentally in *in vitro* and *in vivo* models.

In conclusion, we demonstrated that Aoc3 deficient mice are more prone to both DSS-induced colitis and colonic tumorigenesis. Further studies are needed to elucidate the pathogenesis and evaluate Aoc3 activation as a treatment modality.

Conflicts of Interest

The Authors have no relationship with, or financial interest in any commercial companies pertaining to this article.

Authors' Contributions

A.A. designed the study. Ö.Ö., Ö.A. and A.A. carried out the experiments. Ö.Ö. did the statistical analyses. A.A. wrote the manuscript with support from Ö.Ö. and Ö.A. All Authors discussed the results and contributed to the final manuscript.

Acknowledgements

The Authors are grateful to Dr. Sarp Uzun for reading the manuscript and his advice. Özge Özcan was supported as an intern researcher by The Scientific and Technological Research Council of Turkey (TUBITAK) Project No: SBAG-120S967.

References

1 Strober W, Fuss I, Mannon P: The fundamental basis of inflammatory bowel disease. J Clin Invest 117(3): 514-521, 2007. DOI: 10.1172/JCI30587

2 Ramos GP, Papadakis KA: Mechanisms of disease: inflammatory bowel diseases. Mayo Clin Proc 94(1): 155-165, 2019. DOI: 10.1016/j.mayocp.2018.09.013

3 Shah SC, Itzkowitz SH: Colorectal cancer in inflammatory bowel disease: mechanisms and management. Gastroenterology 162(3): 715-730.e3, 2022. DOI: 10.1053/j.gastro.2021.10.035

4 Cancer Genome Atlas Network: Comprehensive molecular characterization of human colon and rectal cancer. Nature 487(7407): 330-337, 2012. DOI: 10.1038/nature11252

5 Klinman JP: New quinocofactors in eukaryotes. J Biol Chem 271(44): 27189-27192, 1996. DOI: 10.1074/jbc.271.44.27189

6 Finney J, Moon HJ, Ronnebaum T, Lantz M, Mure M: Human copper-dependent amine oxidases. Arch Biochem Biophys 546: 19-32, 2014. DOI: 10.1016/j.abb.2013.12.022

7 Salmi M, Jalkanen S: Vascular adhesion protein-1: a cell surface amine oxidase in translation. Antioxid Redox Signal 30(3): 314-332, 2019. DOI: 10.1089/ars.2017.7418

8 Stolen CM, Marttila-ichihara F, Koskinen K, Yegutkin GG, Turja R, Bono P, Skurnik M, Hänninen A, Jalkanen S, Salmi M: Absence of the endothelial oxidase AOC3 leads to abnormal leukocyte traffic *in vivo*. Immunity 22(1): 105-115, 2005. DOI: 10.1016/j.immuni.2004.12.006

9 Kurkijärvi R, Adams DH, Leino R, Möttönen T, Jalkanen S, Salmi M: Circulating form of human vascular adhesion protein-1 (VAP-1): increased serum levels in inflammatory liver diseases. J Immunol 161: 1549-1557, 1998.

10 Ward ST, Weston CJ, Shepherd EL, Hejmadi R, Ismail T, Adams DH: Evaluation of serum and tissue levels of VAP-1 in colorectal cancer. BMC Cancer 16: 154, 2016. DOI: 10.1186/s12885-016-2183-7

11 Ahmad Zawawi SS, Mohd Azram NAS, Sulong S, Zakaria AD, Lee YY, Che Jalil NA, Musa M: Identification of AOC3 and LRRC17 as colonic fibroblast activation markers and their potential roles in colorectal cancer progression. Asian Pac J Cancer Prev 24(9): 3099-3107, 2023. DOI: 10.31557/APJCP.2023.24.9.3099

12 Koutroubakis IE, Petinaki E, Vardas E, Dimoulios P, Roussomoustakaki M, Maniatis AN, Kouroumalis EA: Circulating soluble vascular adhesion protein 1 in patients with inflammatory bowel disease. Eur J Gastroenterol Hepatol 14(4): 405-408, 2002. DOI: 10.1097/00042737-200204000-00012

13 Chassaing B, Aitken JD, Malleshappa M, Vijay-Kumar M: Dextran sulfate sodium (DSS)-induced colitis in mice. Curr Protoc Immunol 104: 15.25.1-15.25.14, 2014. DOI: 10.1002/0471142735.im1525s104

14 Kiesler P, Fuss IJ, Strober W: Experimental models of inflammatory bowel diseases. Cell Mol Gastroenterol Hepatol 1(2): 154-170, 2015. DOI: 10.1016/j.jcmgh.2015.01.006

15 Tanaka T, Kohno H, Suzuki R, Yamada Y, Sugie S, Mori H: A novel inflammation-related mouse colon carcinogenesis model induced by azoxymethane and dextran sodium sulfate. Cancer Sci 94(11): 965-973, 2003. DOI: 10.1111/j.1349-7006.2003.tb01386.x

16 Bissahoyo A, Pearsall RS, Hanlon K, Amann V, Hicks D, Godfrey VL, Threadgill DW: Azoxymethane is a genetic background-dependent colorectal tumor initiator and promoter in mice: effects of dose, route, and diet. Toxicol Sci 88(2): 340-345, 2005. DOI: 10.1093/toxsci/kfi313

17 Stastna M, Janeckova L, Hrckulak D, Kriz V, Korinek V: Human colorectal cancer from the perspective of mouse models. Genes (Basel) 10(10): 788, 2019. DOI: 10.3390/genes10100788

18 Zeineldin M, Neufeld KL: More than two decades of Apc modeling in rodents. Biochim Biophys Acta 1836(1): 80-89, 2013. DOI: 10.1016/j.bbcan.2013.01.001

19 Zeineldin M, Neufeld KL: New insights from animal models of colon cancer: inflammation control as a new facet on the tumor suppressor APC gem. Gastrointest Cancer Targets Ther 5: 39-52, 2015. DOI: 10.2147/GICTT.S51386

20 Vakal S, Jalkanen S, Dahlström KM, Salminen TA: Human copper-containing amine oxidases in drug design and development. Molecules 25(6): 1293, 2020. DOI: 10.3390/molecules25061293

21 Gok A, Işik A, Bakir S, Uzun S, Guner G, Ozcan O, Cerci B, Onbaşilar I, Akyol A: Role of reduced Bdnf expression in novel Apc mutant allele-induced intestinal and colonic tumorigenesis in mice. In Vivo 37(4): 1562-1575, 2023. DOI: 10.21873/invivo.13241

22 Laroui H, Ingersoll SA, Liu HC, Baker MT, Ayyadurai S, Charania MA, Laroui F, Yan Y, Sitaraman SV, Merlin D: Dextran sodium sulfate (DSS) induces colitis in mice by forming nano-lipocomplexes with medium-chain-length fatty acids in the colon. PLoS One 7(3): e32084, 2012. DOI: 10.1371/journal.pone.0032084

23 Pannecoeck R, Serruys D, Benmeridja L, Delanghe JR, van Geel N, Speeckaert R, Speeckaert MM: Vascular adhesion protein-1: Role in human pathology and application as a biomarker. Crit Rev Clin Lab Sci 52(6): 284-300, 2015. DOI: 10.3109/10408363.2015.1050714

24 Danielli M, Thomas RC, Quinn LM, Tan BK: Vascular adhesion protein-1 (VAP-1) in vascular inflammatory diseases. Vasa 51(6): 341-350, 2022. DOI: 10.1024/0301-1526/a001031

25 Li H, Du S, Niu P, Gu X, Wang J, Zhao Y: Vascular adhesion protein-1 (VAP-1)/semicarbazide-sensitive amine oxidase (SSAO): a potential therapeutic target for atherosclerotic cardiovascular diseases. Front Pharmacol 12: 679707, 2021. DOI: 10.3389/fphar.2021.679707

26 Iffiú-Soltész Z, Bour S, Tercé F, Collet X, Szökő E, Carpéné C: Hypercholesterolemia of obese mice with deletion of vascular adhesion protein-1 occurs without other atherosclerosis risk factor. Vessel Plus 5: 16, 2021. DOI: 10.20517/2574-1209.2021.12

27 Filip A, Taleb S, Bascetin R, Jahangiri M, Bardin M, Lerognon C, Fève B, Lacolley P, Jalkanen S, Mercier N: Increased atherosclerotic plaque in AOC3 knock-out in ApoE(–/–) mice and characterization of AOC3 in atherosclerotic human coronary arteries. Front Cardiovasc Med 9: 848680, 2022. DOI: 10.3389/fcvm.2022.848680

28 Weston CJ, Shepherd EL, Claridge LC, Rantakari P, Curbishley SM, Tomlinson JW, Hubscher SG, Reynolds GM, Aalto K, Anstee QM, Jalkanen S, Salmi M, Smith DJ, Day CP, Adams DH: Vascular adhesion protein-1 promotes liver inflammation and drives hepatic fibrosis. J Clin Invest 125(2): 501-520, 2015. DOI: 10.1172/JCI73722

29 Jargaud V, Bour S, Tercé F, Collet X, Valet P, Bouloumié A, Guillemot JC, Mauriège P, Jalkanen S, Stolen C, Salmi M, Smith DJ, Carpéné C: Obesity of mice lacking VAP-1/SSAO by Aoc3 gene deletion is reproduced in mice expressing a mutated vascular adhesion protein-1 (VAP-1) devoid of amine oxidase activity. J Physiol Biochem 77(1): 141-154, 2021. DOI: 10.1007/s13105-020-00756-y

30 Kinchen J, Chen HH, Parikh K, Antanaviciute A, Jagielowicz M, Fawkner-Corbett D, Ashley N, Cubitt L, Mellado-Gomez E, Attar M, Sharma E, Wills Q, Bowden R, Richter FC, Ahern D, Puri KD, Henault J, Gervais F, Koohy H, Simmons A: Structural remodeling of the human colonic mesenchyme in inflammatory bowel disease. Cell 175(2): 372-386.e17, 2018. DOI: 10.1016/j.cell.2018.08.067

31 Hsia LT, Ashley N, Ouaret D, Wang LM, Wilding J, Bodmer WF: Myofibroblasts are distinguished from activated skin fibroblasts by the expression of AOC3 and other associated markers. Proc Natl Acad Sci U.S.A. 113(15): E2162-E2171, 2016. DOI: 10.1073/pnas.1603534113

32 Jarnicki AG, Schilter H, Liu G, Wheeldon K, Essilfie AT, Foot JS, Yow TT, Jarolimek W, Hansbro PM: The inhibitor of semicarbazide-sensitive amine oxidase, PXS-4728A, ameliorates key features of chronic obstructive pulmonary disease in a mouse model. Br J Pharmacol 173(22): 3161-3175, 2016. DOI: 10.1111/bph.13573

33 Newsome PN, Sanyal AJ, Neff G, Schattenberg JM, Ratziu V, Ertle J, Link J, Mackie A, Schoelch C, Lawitz E, BI 1467335 NASH Phase IIa trial team: A randomised Phase IIa trial of amine oxidase copper-containing 3 (AOC3) inhibitor BI 1467335 in adults with non-alcoholic steatohepatitis. Nat Commun 14(1): 7151, 2023. DOI: 10.1038/s41467-023-42398-w

Received April 21, 2024
Revised May 28, 2024
Accepted May 29, 2024